Probability of Delamination Detection for CFRP DCB Specimens Using Rayleigh Distributed Optical Fiber Sensors

Francesco Falcetelli[1,2(✉)], Demetrio Cristiani[2,3], Nan Yue[2,4], Claudio Sbarufatti[3], Raffaella Di Sante[1], and Dimitrios Zarouchas[2,4]

[1] Department of Industrial Engineering, University of Bologna, 47121 Forlì, Italy
francesco.falcetelli@unibo.it
[2] Faculty of Aerospace Engineering, Delft University of Technology, Delft 2629 HS, The Netherlands
[3] Dipartimento di Meccanica, Politecnico di Milano, 20156 Milano, Italy
[4] Center of Excellence in Artificial Intelligence for Structures, Prognostics and Health Management, Faculty of Aerospace Engineering, Delft 2629HS, The Netherlands

Abstract. Distributed Optical Fiber Sensors (DOFS) show several inherent benefits with respect to conventional strain-sensing technologies and represent a key technology for Structural Health Monitoring (SHM). Despite the solid motivation behind DOFS-based SHM systems, their implementation for real-time structural assessment is still unsatisfactory outside academia. One of the main reasons is the lack of rigorous methodologies for uncertainty quantification, which hinders the performance assessment of the monitoring system. The concept of Probability of Detection (POD) should function as the guiding light in this process, but precautions must be taken to apply this concept to SHM, as it has been originally developed for Non-Destructive Evaluation techniques. Although DOFS have been the object of numerous studies, a well-established methodology for their performance evaluation in terms of PODs is still missing. In the present work, the concept of Probability of Delamination Detection (POD^2) is proposed for a DOFS network; Carbon Fiber-Reinforced Polymers (CFRP) Double-Cantilever Beam (DCB) specimens equipped with DOFS have been tested under static loading, and the strain patterns along with the relative observed delamination size have been collected to generate an adequate database for the POD analysis, suggesting a reference methodology to quantify the performance of DOFS for delamination detection.

Keywords: Structural health monitoring · Probability of detection · Delamination · Distributed optical fiber sensors · Carbon fiber-reinforced polymers

1 Introduction

Over the last decades, composite laminates have become the predominant structural material in a variety of different engineering applications. Nowadays, the quest to develop

P. Rizzo and A. Milazzo (Eds.): EWSHM 2022, LNCE 254, pp. 917–926, 2023.
https://doi.org/10.1007/978-3-031-07258-1_92

safer and lighter structures is still fostering the scientific community to investigate different damage mechanisms in composite materials and their reciprocal interaction. Despite this impressive amount of research, open questions are still present, and the gap toward a complete understanding of the physics behind failure modes in composites has not been bridged yet [1]. The use of large safety factors mitigates the risks of structural failure but often is not deemed sufficient to guarantee safety. Therefore, the development of Structural Health Monitoring (SHM) strategies capable to assess the health status of a particular structural component becomes relevant. Moreover, the considerable amount of information generated by SHM can contribute to deepening the understanding of several damage mechanisms and promote the introduction of innovative composite materials and structures [2].

Despite the interest in the field of SHM has been constantly increasing in the last decades, its industrial implementation is still confined to a restricted number of applications [3]. The lack of well-established methodologies for performance evaluation in terms of damage detection is considered one of the main reasons for this slow transition from academia towards the industry. In NDE the performance of a certain inspecting technique can be evaluated following the guidelines provided in the MIL-HKBK-1823A [4]. Specifically, damage detection capability is quantified using Probability of Detection (POD) curves and Probability of False Alarm (PFA).

However, the naïve application of the POD definition in SHM would lead to untrustworthy results. One of the most important differences between NDE and SHM is their variability sources. In NDE the human factor represents the highest variability contribution. On the other hand, SHM is affected by both temporal and spatial sources of variability, which require more sophisticated statistical tools to generate reliable POD curves.

In a recent literature review carried out by the authors [5], it is shown that a gradual transition towards the use of these specific statistical methods for SHM, such as the Length at Detection (LaD) and the REpeated Measures Random Effects Model (REM^2), is occurring. However, these advancements are not equally distributed among the different sensing technologies available in SHM.

There are several Guided Lamb Waves (GLW) studies that employ model-assisted POD curves to assess the capability of the system in terms of damage detection for different types of structures and damage mechanisms [6–11]. Moreover, GLW based on the time-reversal methodologies [12] can provide POD maps without a data baseline. The performance of Comparative Vacuum Monitoring (CVM) was evaluated using the LaD method [13]. On the other hand, there is a little amount of literature regarding the performance evaluation of systems based on Optical Fiber Sensors (OFS) using POD curves. Grooteman developed a numerical model of a 3-stringer thermoplastic composite panel with fiber Bragg gratings (FBGs) installed on it and computed the frequency shift in the eigenmodes. They developed a POD curve using the hit/miss approach and the modal strain energy as damage indicator [14]. Sbarufatti et al. developed POD curves to quantify the performance of FBGs bonded onto an aluminum stiffened panel in terms of minimum detectable crack length [15].

OFS can be embedded in composites and also in 3D printed structures [16]. They have been successfully used in several SHM applications and recently they proved to be

a valid alternative to accelerometers for modal analysis [17]. In particular, distributed sensing based on Raman, Brillouin [18], and Rayleigh backscattering, is particularly promising since it allows to collect a larger amount of data and increases the sensor network density on the structure. At the current state of the art, to the best of the authors' knowledge, there are no studies qualifying DOFS using statistical tools such as POD curves [5]. It is reasonable to expect that DOFS might be more sensitive to certain kinds of damage and less sensitive to others. Therefore, for composite laminates different POD curves are expected depending on the damage mechanism involved, suggesting that DOFS performance should be evaluated referring to each specific failure mode. For example, delamination is a very common interlaminar damage mechanism and can also occur in adhesive bonds [19].

This study aims to make a first step towards the qualification of DFOS installed in composite structures. In this perspective, DOFS are applied to Carbon Fiber-reinforced polymers (CFRP) double cantilever beam (DCB) specimens under Mode I quasi-static loading. Probability of Delamination Detection (POD^2) curves are developed and then used as metrics to evaluate the performance of the monitoring system.

2 Methodology

2.1 Specimens Manufacturing

The manufacturing of five DCB coupons was carried out following the guidelines described in the ASTM D5528 standard [20]. A square panel with a side length of 300 mm was manufactured by hand layup, laminating AS4 HexPly 8552® unidirectional carbon prepregs with $[0_{24}]$ stacking sequence. The initiation site for delamination was created by inserting a Teflon™ film at the midplane of the panel such that an initial crack length of 50 mm was obtained. Specimens of width equal to 25 mm were cut from the laminate panel using an automated Proth® cutting machine. The loading blocks were produced matching the specimen width of 25 mm. Potential surface impurities were removed by sandblasting, whereas the surface of the specimen was rubbed with conventional sandpaper. After cleaning with an alcoholic solution, bonding was realized using the 3M™ Scotch-Weld™ EC-9323 structural epoxy adhesive.

2.2 Optical Fiber Sensors

Single mode optical fibers, with ORMOCER® coating developed by FBGS Technologies GmbH, were employed. The fibers were connected through LC/APC connectors to an ODiSI-B interrogator from Luna Innovations Inc. The optical data acquisition system leverages swept-wavelength interferometry to measure the Rayleigh backscatter originating along the fiber due to random fluctuations in the refractive index [21]. When a certain region of the optical fiber experiences strain or temperature variations there is a shift in the reflected spectrum. Analogously to FBGs, this shift can be related back to strain and temperature variations through proper calibration constants. On the other hand, in contrast to FBGs, the spectral shift is computed for each gauge interval, thus allowing distributed sensing. The interrogator was set up with gauge intervals of 0.65 mm and a sampling rate of 23.8 Hz.

2.3 Experimental Setup

Figure 1a shows the expected (analytical and experimental) strain profiles. Figure 1b shows how DOFS were applied on the specimen skin to measure strains along their longitudinal direction. Bonding was realized using the ThreeBond 1742® cyanoacrylate adhesive.

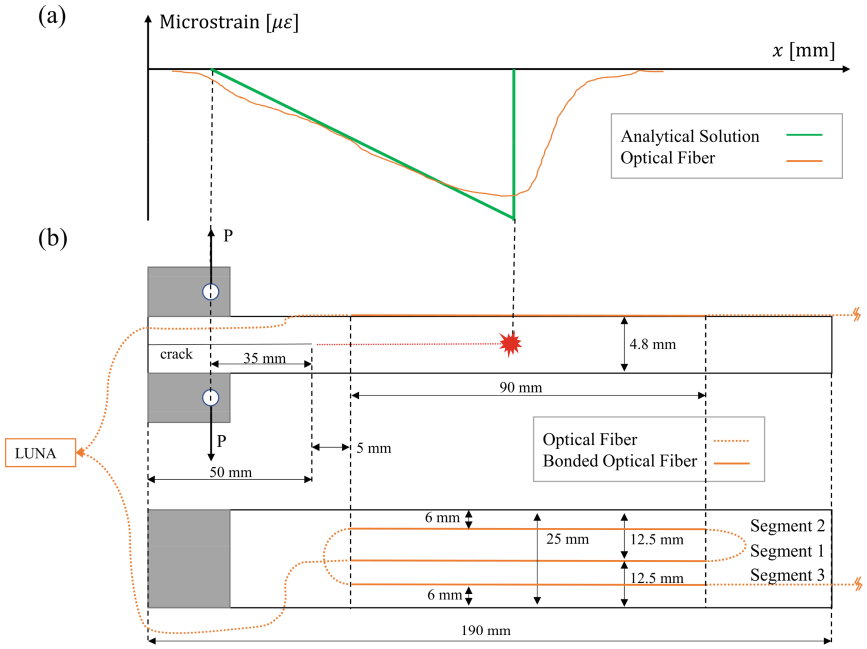

Fig. 1. DCB specimen geometry and the optical fiber layout.

One side of the specimens was coated with white paint and tick marks were made to allow the estimation of the true crack length. Due to the large number of pictures to be visually analyzed it was decided to estimate the true crack length by computing the compliance value C, which is defined as the ratio between the displacement and the applied load in the DCB specimen. Specifically, it was exploited the linear relationship existing between the cube root of compliance, $C^{1/3}$, and the delamination length. The true delamination length at different time steps was estimated for each specimen from a subset of the pictures taken from the camera during the whole test and a least square regression was used to fit the data. This procedure allowed to obtain from the compliance value, which is available at every time step, the crack length, avoiding the expensive task of assessing manually hundreds of images. Photos were made using a 9 Megapixel camera placed in front of the tensile test machine (Zwick - 20 kN), which is visible in Fig. 2. The Zwick software was configured with a displacement rate of 1mm/min to synchronize both the LUNA system and the camera car with the tensile test machine. Data acquisition was made with a sampling frequency of 0.5 Hz. A total of five DCB

specimens was tested in the experimental campaign ASTM D5528 standard [20], but considering that every specimen has three optical fiber segments, this allows to multiply by three the number of linear regressions used to generate POD curves.

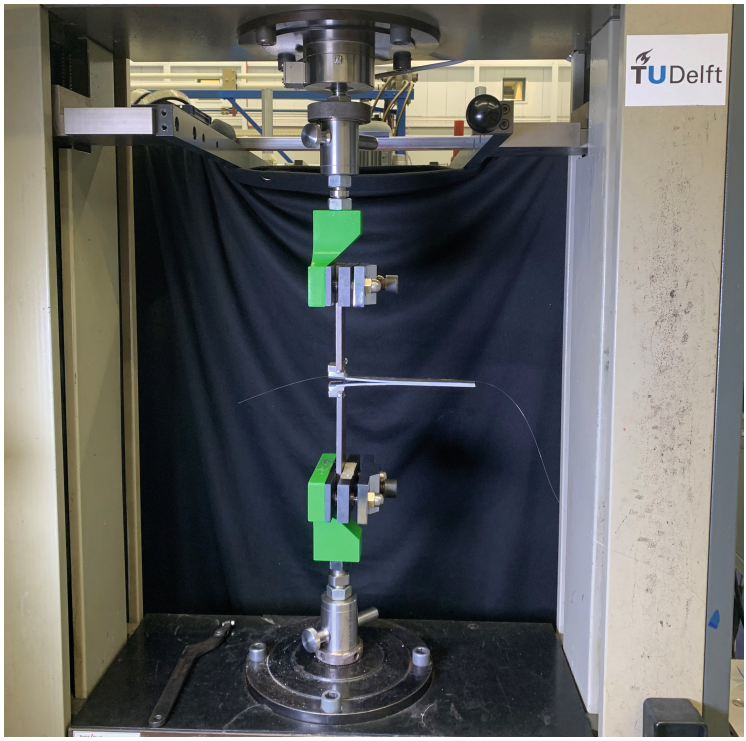

Fig. 2. DCB testing setup.

3 Results

For every segment of each specimen, the ODiSI-B acquired data can be organized in a matrix, S_{xt}, where each row represents the strain evolution along the fiber direction at a certain time-step, t, and each column represents the strain evolution over time at a certain location, x. The plot in Fig. 3 displays several rows of the S_{xt} matrix, to show the typical shapes of the measured strain profiles. The black dots are placed at the lower peaks of each strain profile to highlight the crack tip movement as delamination grows. In every POD study, it is crucial to identify a damage index that is correlated with damage severity. Referring to Fig. 3 it is reasonable to assume that delamination detection can be detected after a few millimeters of crack length. Therefore, for POD^2 purposes, only the first strain profiles are relevant (the others may be useful for the monitoring of crack propagation once detection has been made). A reasonable damage index (DI) is the strain value measured at the crack location (black dots in Fig. 3). However, experimental data

showed that the strain values measured from DOFS at the crack location and the crack length have a non-linear relationship.

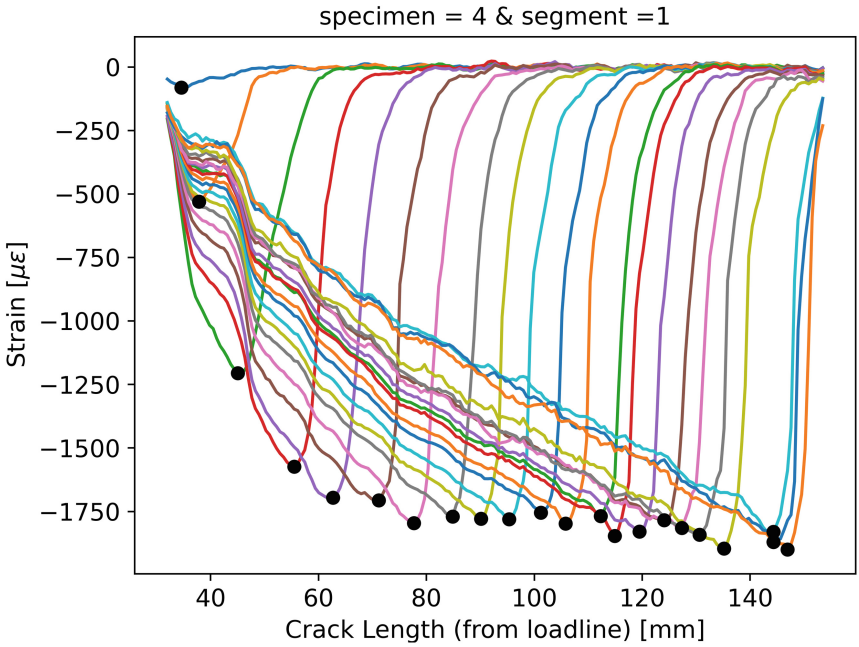

Fig. 3. Measured strain profiles at several delamination lengths.

The linearity between the DI and the crack length is a requirement for the LaD method. A solution is to adopt as DI the natural logarithm of the absolute value of the strain profile measured at the crack tip, as described by Eq. (1):

$$\mathrm{DI} = \ln(|\min(\varepsilon_x)|) \tag{1}$$

where ε_x denotes the strain value along the x-direction, which is the longitudinal direction (see Fig. 1a). The multiple linear regressions performed for each specimen segment using the abovementioned DI are shown in Fig. 4. The x-axis has its zero value in correspondence with the onset of the bonding region of the DOFS segments. Thus, negative crack length values represent crack lengths that have not reached the bonded segment yet. In the literature, there is not a well-established methodology to choose the right threshold line for the LaD method. In this study, the threshold value was determined by adding three standard deviations of the noise level (measured previously from preliminary experiments) to the highest intercept of the regression lines in Fig. 4. This is a conservative approach to determining the detection threshold. An alternative is to select other intercepts with a lower value. However, this would result in several lengths at detection with negative values and is not reasonable from an experimental point of view. Assuming a normal distribution of the various length at detection it is

possible to develop the corresponding POD^2 by applying Eq. 2:

$$POD(a) = Pr(X < a) = \Phi_{norm}((a - \bar{x})/s) \tag{2}$$

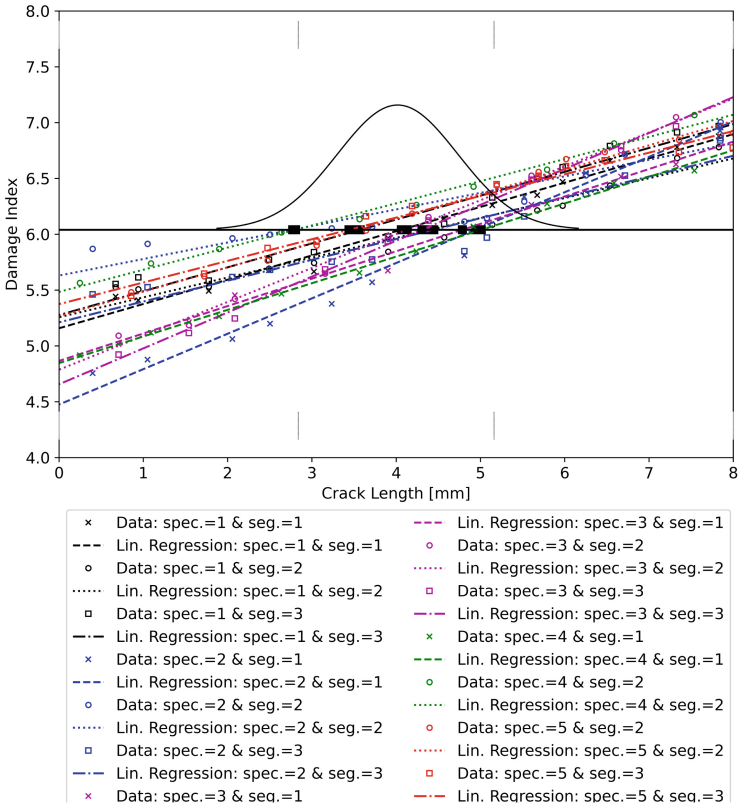

Fig. 4. Length at Detection method applied to DFOS data for crack detection.

where Φ_{norm} is the standard normal cumulative distribution function, $\bar{x}$ is the estimated mean and s is the estimated standard deviation from the lengths at detection. The result is shown in Fig. 5. The critical a_{90} value represents the crack length whose probability of detection equals 90%. However, to qualify the detection performance of DOFS it is more important to refer to the $a_{90/95}$ value. The $a_{90/95}$ denotes the crack length values which can be detected with 90% of probability and 95% of confidence. In other words, $a_{90/95}$ is the abscissa value where the lower bound hits 0.9. It is possible to compute the lower confidence bound of the POD^2 curve using the One-Sided Tolerance Interval (OSTI) approach, which translates in Eq. 3:

$$T = \bar{x} + k(n, \gamma, \alpha) \cdot s \tag{3}$$

where T is the upper bound for a certain quantile of a normally distributed population and k represents the tolerance factor, which in turn depends on the n, γ, and α parameters.

Specifically, n denotes the number of samples (in this case the number of DOFS segments), γ is the desired level of confidence (commonly set to 95%) and α is the coverage level (set to 90%).

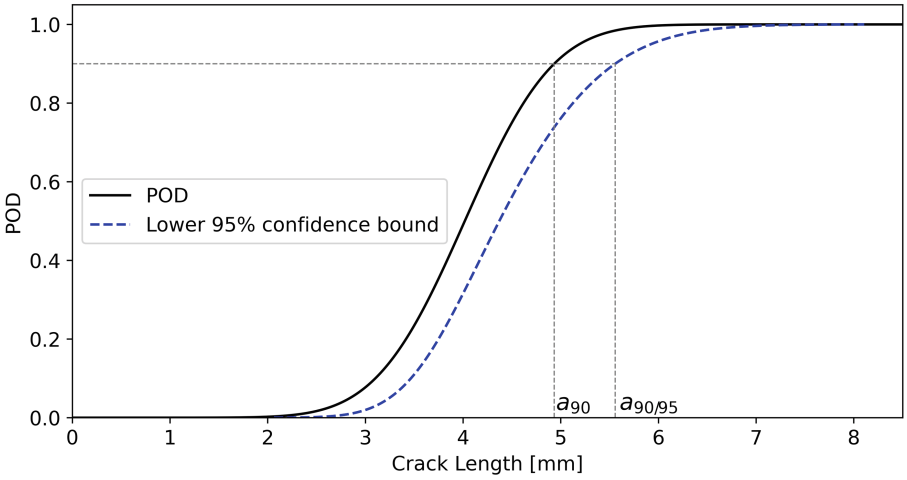

Fig. 5. POD and its lower 95% confidence bound.

The a_{90} and the $a_{90/95}$ shown in Fig. 5 have values of 4.93 mm and 5.56 mm respectively. The difference between a_{90} and $a_{90/95}$ can be considered a measure of the uncertainty involved in the experimental campaign since the lower bound is directly proportional to s. To reduce the $a_{90/95}$ one can increase the number of specimens because k decreases as n increases. On the other hand, increasing n means higher costs and time required to perform the experimental campaign. Therefore, if it is impossible to test more specimens, the only possibility to lower $a_{90/95}$ is to redesign the experimental setup and reduce the involved variability sources to obtain a lower s.

4 Conclusions

In this study, the LaD method has been applied to quantify the performance of DOFS for Mode I delamination detection in CFRP DCB coupons. Once the lower bound of the POD^2 is determined, the $a_{90/95}$ value can be used as a performance metric for DOFS. Its value depends on many factors such as the damage type, number of specimens, specimen material, DOFS interrogator, DOFS coating layers, and the adhesive mechanical properties, which determine the strain transfer properties of the optical fiber [22]. This study showed a first attempt at developing a qualification methodology that can be easily reproduced in other laboratories. While the results obtained in this study are specific to the experimental setup which have been used, the validity of the proposed methodology is general. The transposition of the POD^2 curves to other structures is only possible if the variability sources, the manufacturing process, the applied loads, and the damage mechanisms are the same. For instance, ongoing experimental activity seems to suggest that

delamination occurring in Mode I (which was the subject of this study) has a different POD^2 with respect to Mode II delamination or a mixture between the two modes. This happens because the loading and the boundary conditions are different. Larger structures may be characterized by delamination related to different loading modes. Future research activities would be devoted to the study of damage localization and characterization metrics and to understanding the implications of upscaling the POD^2 curves obtained from simple coupons to more complex geometries. This would be particularly useful since the direct development of POD curves from real structures would be unfeasible due to the huge cost of manufacturing and testing large structures.

References

1. Saeedifar, M., Zarouchas, D.: Damage characterization of laminated composites using acoustic emission: a review. Compos. Part B Eng. **195**, 108039 (2020). https://doi.org/10.1016/j.compositesb.2020.108039
2. Giurgiutiu, V.: Structural Health Monitoring of Aerospace Composites. Elsevier, Amsterdam (2016)
3. Cawley, P.: Structural health monitoring: closing the gap between research and industrial deployment. Struct. Health Monit. **17**, 1225–1244 (2018). https://doi.org/10.1177/1475921717750047
4. Department of Defense Handbook: Nondestructive Evaluation System Reliability Assessment (2009)
5. Falcetelli, F., Yue, N., Di Sante, R., Zarouchas, D.: Probability of detection, localization, and sizing: the evolution of reliability metrics in Structural Health Monitoring. Struct. Health Monit. (2021). https://doi.org/10.1177/14759217211060780
6. Moriot, J., Quaegebeur, N., Le Duff, A., Masson, P.: A model-based approach for statistical assessment of detection and localization performance of guided wave–based imaging techniques. Struct. Health Monit. **17**, 1460–1472 (2018). https://doi.org/10.1177/1475921717744679
7. Gianneo, A., Carboni, M., Giglio, M.: Feasibility study of a multi-parameter probability of detection formulation for a Lamb waves–based structural health monitoring approach to light alloy aeronautical plates. Struct. Health Monit. Int. J. **16**, 225–249 (2017). https://doi.org/10.1177/1475921716670841
8. Liu, C., Dobson, J., Cawley, P.: Efficient generation of receiver operating characteristics for the evaluation of damage detection in practical structural health monitoring applications. Proc. R. Soc. Math. Phys. Eng. Sci. **473**, 20160736 (2017). https://doi.org/10.1098/rspa.2016.0736
9. Yue, N., Aliabadi, M.H.: Hierarchical approach for uncertainty quantification and reliability assessment of guided wave-based structural health monitoring. Struct. Health Monit. 147592172094064 (2020). https://doi.org/10.1177/1475921720940642
10. Mariani, S., Rendu, Q., Urbani, M., Sbarufatti, C.: Causal dilated convolutional neural networks for automatic inspection of ultrasonic signals in non-destructive evaluation and structural health monitoring. Mech. Syst. Signal Process. **157**, 107748 (2021). https://doi.org/10.1016/j.ymssp.2021.107748
11. Tschoke, K., et al.: Feasibility of model-assisted probability of detection principles for structural health monitoring systems based on guided waves for fibre-reinforced composites. IEEE Trans. Ultrason. Ferroelectr. Freq. Control 1 (2021). https://doi.org/10.1109/TUFFC.2021.3084898

12. Falcetelli, F., Venturini, N., Romero, M.B., Martinez, M.J., Pant, S., Troiani, E.: Broadband signal reconstruction for SHM: an experimental and numerical time reversal methodology. J. Intell. Mater. Syst. Struct. 1045389X2097247 (2021). https://doi.org/10.1177/1045389X20972474
13. Roach, D.: Real time crack detection using mountable comparative vacuum monitoring sensors. Smart Struct. Syst. **5**, 317–328 (2009). https://doi.org/10.12989/SSS.2009.5.4.317
14. Grooteman, F.P.: Damage detection and probability of detection for a SHM system based on optical fibres applied to a stiffened composite panel. In: Proceedings of the 25th International Conference on Noise and Vibration Engineering, pp. 3317–3330. Katholieke Universiteit Leuven, Leuven, Belgium (2012)
15. Sbarufatti, C., Giglio, M.: Performance qualification of an on-board model-based diagnostic system for fatigue crack monitoring. J. Am. Helicopter Soc. **62**, 1–10 (2017). https://doi.org/10.4050/JAHS.62.042008
16. Falcetelli, F., Di Sante, R., Troiani, E.: Strategies for embedding optical fiber sensors in additive manufacturing structures. In: Rizzo, P., Milazzo, A. (eds.) European Workshop on Structural Health Monitoring. EWSHM 2020. LNCE, vol. 128, pp. 362–371. Springer, Cham (2021). https://doi.org/10.1007/978-3-030-64908-1_34
17. Falcetelli, F., Martini, A., Di Sante, R., Troncossi, M.: Strain modal testing with fiber Bragg gratings for automotive applications. Sensors **22**, 946 (2022). https://doi.org/10.3390/s22030946
18. Bastianini, F., Di Sante, R., Falcetelli, F., Marini, D., Bolognini, G.: Optical fiber sensing cables for Brillouin-based distributed measurements. Sensors **19**, 5172 (2019). https://doi.org/10.3390/s19235172
19. Pascoe, J.A., Alderliesten, R.C., Benedictus, R.: Methods for the prediction of fatigue delamination growth in composites and adhesive bonds–a critical review. Eng. Fract. Mech. **112–113**, 72–96 (2013). https://doi.org/10.1016/j.engfracmech.2013.10.003
20. Standard test method for mode I interlaminar fracture toughness of unidirectional fiber-reinforced polymer matrix composites. ASTM international. ASTM international, West Conshohocken, PA, USA (2007)
21. Gifford, D.K., et al.: Swept-wavelength interferometric interrogation of fiber Rayleigh scatter for distributed sensing applications. In: Fiber Optic Sensors and Applications V, p. 67700F. International Society for Optics and Photonics (2007). https://doi.org/10.1117/12.734931
22. Falcetelli, F., Rossi, L., Di Sante, R., Bolognini, G.: Strain transfer in surface-bonded optical fiber sensors. Sensors **20**, 3100 (2020). https://doi.org/10.3390/s20113100